Ab initio study of the angular dependence of giant magnetoresistance in Fe/Cr superlattices

B. Yu. Yavorsky* and I. Mertig
Institut für Theoretische Physik, Technische Universität Dresden, D-01062 Dresden, Germany

A. Ya. Perlov,* A. N. Yaresko,* and V. N. Antonov*
Max-Planck Institute for Physics of Complex Systems, D-01187 Dresden, Germany
(Received 2 November 1999)

Self-consistent electronic structure calculations for Fe/Cr superlattices with a spiral magnetic configuration were performed by means of a modified linear muffin-tin orbital method. Based on these results calculations of the conductivity as a function of the magnetic configuration and the angular dependence of giant magnetoresistance have been performed. Different magnetic configurations such as spiral structures and tilting modes are compared at the level of total energy and GMR.

I. INTRODUCTION

There is currently significant interest in artificially layered magnetic structures. It was mainly caused by the discovery of interlayer exchange coupling (IXC)[1] and giant magnetoresistance (GMR) in Fe/Cr(001) superlattices.[2,3] It was found that the electrical resistivity of the system with antiferromagnetically (*A*) coupled successive iron layers drops strongly when the magnetic moments of adjacent Fe layers are aligned ferromagnetically (*F*) by an external magnetic field. A large amount of theoretical interpretations of GMR consider diffusive spin-dependent electron scattering being the source of the effect. These calculations assume mostly a free-electron dispersion for the multilayer.[4–6] Based on these models the experimental results have been analyzed to distinguish between the influence of bulk or interface scattering.[7,8] At the same time several authors[9–11] showed the important role of the detailed electronic structure of the superlattice as a function of the magnetic configuration for the explanation of the GMR effect. These calculations take the coherent scattering of the electrons in the superlattice potential into account, in particular, the coherent scattering of the electrons at the potential steps of the interfaces between magnetic and spacer layers but neglect spin-dependent impurity scattering. Within this approach was shown that the drop of the resistivity can also be caused by the change of the Fermi velocities[11] as a function of the magnetic configuration. In real samples both effects are superimposed and their influence can not be separated.

Until now most of the theoretical investigations of GMR in superlattices were restricted to considerations of collinear, *A* and *F*, magnetic configurations. The variation of the effect with changing angle between the layer magnetizations was studied within model approaches[12,13] and only once by using a fully relativistic spin-polarized screened KKR method for a Co/Cu trilayer.[14] Experiments have found for the most part simple $\cos\alpha$ behavior for the changes of the current-in-plane (CIP) GMR signal with the angle α between the layer magnetizations;[15] however, for the current perpendicular to the plane of the layers (CPP), significant deviations have been established.[16,17]

Another important motivation for the investigation of noncollinear magnetic configurations are recent polarized neutron spectrometry measurements in Fe/Cr superlattices.[18] The authors discuss the existence of noncollinear exchange coupling of the Fe layers caused by a spiral modulation of the Cr moments. Based on these results, we assume the existence of noncollinear magnetic order in the Fe/Cr superlattice. The mechanism of formation and stabilization of helical spin-density waves is discussed elsewhere.[19] For a review see also Pierce *et al.*[20] and Zabel.[21]

Recently the traditional band structure calculation methods[22] and the local spin-density approximation (LSDA)[23] were extended to the case of non-collinear magnetic systems. A review of the method including current applications is given by Sandratskii.[24] The approach was proven to yield reliable results for various properties of magnetic materials. In particular, a successful application to study magnon dynamics in ferromagnetic metals was presented using a modified linear muffin-tin orbital method (LMTO).[25] The same modified LMTO method was used in this paper to study the angular dependence of GMR in Fe/Cr superlattices.

II. ELECTRONIC STRUCTURE OF SPIN SPIRALS AND TRANSPORT IN NONCOLLINEAR MAGNETS

Starting from now, we shall assume that in the materials under consideration the spin-orbit interaction can be neglected. Under this assumption the spatial and the spin variables are independent. For noncollinear magnets at certain atomic position t there is the local magnetization axis given by the spherical angles φ_t, θ_t with respect to the global coordinate system. In this case the spin functions will be of the form[26]

$$\tilde{\chi}_1^t = \begin{pmatrix} \cos(\theta_t/2)\exp(-i\varphi_t/2) \\ \sin(\theta_t/2)\exp(i\varphi_t/2) \end{pmatrix},$$
$$\tilde{\chi}_2^t = \begin{pmatrix} -\sin(\theta_t/2)\exp(-i\varphi_t/2) \\ \cos(\theta_t/2)\exp(i\varphi_t/2) \end{pmatrix}. \quad (1)$$

Although the spatially varying spin direction in general leads to the loss of the translational invariance of the crystal lat-

tice, the particular case of the spiral spin structures, also called simple spin density waves (SDW),[26] allows a straightforward generalization of the traditional band structure calculation methods. The magnetic configuration of a SDW is determined by a constant vector of the spiral **q**. For two equivalent atomic positions t and t', separated by the lattice translation **R**, mutual directions of the magnetization axes obey the condition

$$\varphi_{t'}=\varphi_t+\mathbf{qR}, \quad \theta_{t'}=\theta_t; \quad \mathbf{R}=\mathbf{r}_{t'}-\mathbf{r}_t. \tag{2}$$

This condition allows the generalization of the Bloch theorem to the crystals with spiral magnetic configuration by introducing instead of the usual lattice translation $T_{\mathbf{R}}$ a new operator $\tilde{T}^{\mathbf{q}}_{\mathbf{R}}$ (Ref. 27)

$$\tilde{T}^{\mathbf{q}}_{\mathbf{R}}=U(\mathbf{qR})T_{\mathbf{R}}, \quad \tilde{T}^{\mathbf{q}}_{\mathbf{R}}\tilde{\psi}^{\mathbf{k}}(\mathbf{r})=\exp(i\mathbf{kr})\tilde{\psi}^{\mathbf{k}}(\mathbf{r}), \tag{3}$$

where $U(\varphi)$ is the operator of the spin rotation by angle φ around the axis of the spiral and $\tilde{\psi}^{\mathbf{k}}(\mathbf{r})$ are the Bloch functions of the system. **k** is the Bloch vector. It was shown[22] on the basis of the generalized Bloch theorem that the modification of the band structure calculation methods leads to a secular equation which dimension for both commensurate and noncommensurate spin spirals is only two times larger than for collinear magnets. In particular, the modification of the LMTO formalism[25] requires the substitution of the standard LMTO structure constants $S^{\mathbf{k}}_{tL,t'L'}$ (Ref. 28) by the new ones $\tilde{S}^{\mathbf{k,q}}_{tL,t'L'}$ which are expressed through $S^{\mathbf{k-q/2}}_{tL,t'L'}$ and $S^{\mathbf{k+q/2}}_{tL,t'L'}$.

The collinear F and A magnetic configurations can be regarded as particular cases of the spin spirals. The ferromagnetic order corresponds simply to $\mathbf{q}=0$. The electronic structure of an antiferromagnet can be calculated as a commensurate magnetic spiral with a spiral vector of length $q=\pi/c$ directed along one of the basis translational vectors **c**. Next, with $\theta_t=90°$ one obtains a magnetic configuration where all atomic layers normal to **c** are intrinsically ferromagnetic. Under these conditions any fixed spiral vector with a length $0\leqslant q\leqslant \pi/c$ corresponds to a certain constant value of the angle $0\leqslant\alpha\leqslant 180°$ between the layer magnetizations. So, carrying out the electronic structure calculations for a set of spiral vectors, we can study the dependence of the transport properties on the angle between the layer magnetizations α.

The transport properties are calculated by means of a linearized Boltzmann equation in relaxation time approximation

$$-e\left(\frac{\partial f^o_k}{\partial \epsilon_k(\alpha)}\right)\mathbf{v}_k(\alpha)\mathbf{E}=\frac{g_k(\alpha)}{\tau}. \tag{4}$$

The Boltzmann equation is an integral equation to determine the deviation of the electron distribution function $g_k(\alpha)$ from the Fermi-Dirac equilibrium distribution f^o_k if an external electric field **E** is applied. $\mathbf{v}_k(\alpha)$ is the velocity of the electrons. The scattering of the electrons is described by means of an isotropic relaxation time τ. e is the charge of the electron and k is a short-hand notation for wave vector **k** and band index ν.

With the current density

$$\mathbf{j}(\alpha)=2e\sum_k \mathbf{v}_k(\alpha)g_k(\alpha) \tag{5}$$

and Ohm's law

$$\mathbf{j}(\alpha)=\hat{\sigma}(\alpha)\mathbf{E} \tag{6}$$

the conductivity tensor becomes

$$\hat{\sigma}(\alpha)=2e^2\tau\sum_k \delta[\epsilon_k(\alpha)-\epsilon_f]\mathbf{v}_k(\alpha)\otimes\mathbf{v}_k(\alpha). \tag{7}$$

Obviously, the conductivity tensor reflects the electronic and magnetic structure of the multilayer via the dispersion law $\epsilon_k(\alpha)$, the Fermi velocities $\mathbf{v}_k(\alpha)$ and Fermi surface $\epsilon_k(\alpha)=\epsilon_f$. It has to be mentioned that the influence of an external magnetic field via a Lorentz force which would cause normal magnetoresistance is not included in the calculation [see Eq. (4)]. The influence of an external magnetic field that changes the relative orientation of the layer magnetizations and causes GMR in magnetic multilayers, however, enters the calculation via the electronic structure. Consequently, the GMR ratio

$$\mathrm{GMR}(\alpha)=\frac{\sigma(0)-\sigma(\alpha)}{\sigma(\alpha)} \tag{8}$$

can be calculated as a function of α. Under the assumption that an increasing external magnetic field changes the relative orientation of the layer magnetizations continuously $\mathrm{GMR}(\alpha)$ describes the field dependence of the GMR ratio.

Because of the tetragonal symmetry of the considered multilayers the conductivity tensor consists of two different components. $\sigma_{xx}=\sigma_{yy}$ is the in-plane conductivity and causes CIP-GMR, whereas σ_{zz} is the conductivity perpendicular to the planes and causes CPP-GMR.

Since the relaxation time which describes the scattering in the system was assumed to be constant from the very beginning [Eq. (4)] the GMR ratio is independent on τ. This is a quite rough approximation. As it was shown by Binder *et al.*[29] the relaxation time τ^{σ}_k is in general strongly spin σ and state k dependent in layered structures. This influences of course the absolute values of the conductivities and the GMR ratio. With the present calculations we would like to demonstrate that the experimentally obtained functional dependence with respect to the relative angle between the orientations of the layer magnetizations is determined by the electronic structure of the layered system. Spin-dependent bulk or interface scattering would modify the absolute values but not the functional dependence.

III. DETAILS OF CALCULATION

We have studied a superlattice with six atomic layers of iron followed by six chromium monolayers along (001) direction of the bcc lattice with $a=2.87$ Å. The symmetry of this system corresponds to the tetragonal group D_{4h}. The thickness of the Cr layer (8.6 Å) was chosen close to the experimental value of the so-called first antiferromagnetic maximum of the IXC.[30] The magnetic moments of both iron and chromium were supposed to be parallel to the multilayer plane. The Fe individual layers were assumed to be intrinsi-

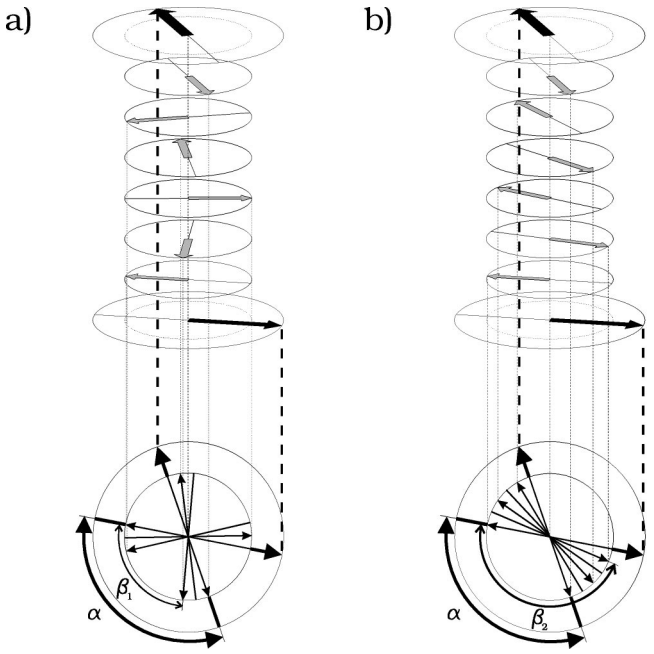

FIG. 1. Relative orientation of the magnetic moments in 6Fe/6Cr superlattices for the angle of coupling between the Fe layers $\alpha=120°$ and for the angle between the Cr layer magnetization (a) $\beta_1=96°$ and (b) $\beta_2=168°$. The black arrows correspond to the moments of Fe and the grey arrows to the moments of Cr.

cally ferromagnetic. The calculations were carried out for seven values of the spin-spiral vectors **q** along (001) direction, so that the angle α between the magnetizations of the successive Fe individual layers increase from 0 (F coupling) up to 180° (A coupling) with steps of 30°. For the distribution of the magnetic moments inside the Cr individual layer we have chosen the model suggested in Ref. 18. Namely, the Cr at the interfaces assumed to be *A* coupled with the Fe layers, while inside the layer the angle of Cr-Cr coupling was fixed to a constant value β. Under this boundary condition for each value α occur in general five different values of β, with $\Delta\beta=72°$. As an example Fig. 1 shows the magnetic configurations for the case $\alpha=120°$ and the two values of β ($\beta_1=96°, \beta_2=168°$). For both collinear configurations, $\alpha=0$ and $\alpha=180°$, exist only three nonequivalent values of β.

The self-consistent LMTO band structure calculations were carried out at a grid of 5760 **k** points in the Brillouin zone. All **k**-integrations have been performed by the tetrahedron method.[31] For the calculations of the conductivity tensor 22528 **k** points have been used.

IV. RESULTS AND DISCUSSION

The current-in-plane and the current-perpendicular-to-plane components of $\hat{\sigma}$ along with the densities of states at the Fermi level, the absolute values of magnetic moment averaged over all Cr monolayers, and the total energies are compiled in Table I.

A. Magnetic moments and total energy

Comparing the total energy the ground state of the system corresponds to antiferromagnetic coupling between the iron layers and an intrinsically antiferromagnetic chromium layer. The total energy of this configuration was chosen to be zero. The values of the magnetic moments are in this case close to the ones of the pure constituents. The change of the magnetic order in the Cr layer from collinear to noncollinear leads to a considerable increase of the total energy by more than 1.5 mRy per unit cell. The energy difference between the less favorable configurations, however, is very small which can be understood in terms of the strongly reduced Cr moments. The Cr moments of the noncollinear configurations are more than two times smaller. At the same time the density of states at the Fermi level increases.

These features are qualitatively reproduced for all other values of the angle α of Fe-Fe coupling. In each case the magnetic configuration with the smallest total energy reflects the tendency for chromium moments to be coupled antiferromagnetically (under the above mentioned boundary conditions). In addition, the favorable angle β between chromium magnetizations is distinguished by the smallest value of the density of states at the Fermi level and the largest values of the chromium moments. At the same time along with the change of the coupling between the iron layers from *A* to *F* the absolute values of the Cr moments are substantially diminished. Due to this tendency the differences between all calculated data at fixed α and various β decrease, and in the ferromagnetic configuration the system is nearly frustrated with respect to the orientation of the chromium moments.

In the following we concentrate on magnetic configurations with the smallest total energy at fixed angle of Fe-Fe coupling. Figure 2(a) shows the distribution of the absolute values of the magnetic moments in 6Fe/6Cr superlattices with collinear ferromagnetic, antiferromagnetic, and a noncollinear configuration ($\alpha=60°$). In the middle of the Fe layer there are four atomic layers with the value of the magnetic moment close to the one of bulk iron. Among one another these moments differ by less than $0.03\mu_B$. At the interface occurs appreciable charge transfer from iron to chromium which is accompanied by a decrease of the Fe moment and at the same time an increase of the Cr moment. For antiferromagnetic coupling ($\alpha=180°$) the Cr moments are nearly constant and maximal in comparison to other configurations. At $\alpha=60°$ the Cr moments are reduced to half size and are suppressed for $\alpha=0$. Due to the even number of atomic Cr layers and the ideally sharp interfaces the formation of an antiferromagnetic Cr state is impossible. Consequently, Cr tends to be nonmagnetic. At the interface certain appreciable values of magnetic Cr moments are preserved by the strong exchange interaction with iron, while at the middle of the Cr layer the moments go down and at the center there is a minimum with an absolute value close to zero. The overall tendency of the decrease of the magnetic moments along with the changing of the angle of coupling from 180° to 0 can be seen from Fig. 2(b). The values of magnetic moments in the middle of the Fe layer are mostly determined by the strong Fe-Fe interaction and are almost unchanged (they are not shown). The interface Fe moment decreases smoothly by $0.085\mu_B$ while for the Cr atoms at the interface and at the center of the layer these changes are $0.35\mu_B$ and $0.5\mu_B$, respectively.

The dependence of the total energy on the angle of Fe-Fe coupling is shown in Fig. 3. The energy difference between

TABLE I. Calculated data for 6Fe/6Cr(001) superlattices with a spiral magnetic order. Asterisks indicate energetically favorable configurations for each value of the angle of Fe-Fe coupling.

Fe-Fe angle α [deg]	Cr-Cr angle β [deg]	$\sigma_{\mathbf{cpp}}$ [a.u.]	$\sigma_{\mathbf{cip}}$ [a.u.]	$N(E_f)$ [states/(Ry atom)]	$\langle \mathbf{m}_{\mathbf{Cr}} \rangle$ [μ_B]	ΔE_{tot} [mRy/cell]
180	180*	0.01388	0.04346	13.23050	0.58	0.
	108	0.01910	0.04033	14.58174	0.16	1.79
	36	0.01793	0.04131	15.37726	0.23	1.63
150	318	0.01881	0.04058	14.27062	0.23	1.73
	246	0.01941	0.04030	14.19064	0.16	1.90
	174*	0.01535	0.04225	12.90766	0.56	0.25
	102	0.01986	0.04014	13.92668	0.16	1.93
	30	0.01877	0.04069	14.48649	0.23	1.77
120	312	0.02104	0.04176	12.45971	0.21	1.97
	240	0.02179	0.04176	13.15168	0.15	2.22
	168*	0.01813	0.04085	11.27665	0.50	0.78
	96	0.02255	0.04220	12.72269	0.16	2.13
	24	0.02109	0.04170	12.36733	0.21	2.03
90	306	0.02535	0.04575	12.28913	0.18	2.19
	234	0.02570	0.04563	12.29866	0.13	2.42
	162*	0.02159	0.04308	10.42604	0.42	1.51
	90	0.02659	0.04619	11.82488	0.14	2.28
	18	0.02548	0.04584	11.78713	0.19	2.32
60	300	0.02907	0.05130	11.61043	0.15	2.53
	228	0.02933	0.05157	11.73950	0.12	2.76
	156*	0.02651	0.04940	10.79813	0.32	2.21
	84	0.03015	0.05191	11.25422	0.12	2.69
	12	0.02967	0.05148	11.26654	0.17	2.48
30	294	0.03905	0.05920	11.81828	0.12	2.90
	222	0.03996	0.05961	11.91544	0.11	2.96
	150*	0.03515	0.05718	11.01165	0.22	2.87
	78	0.04002	0.05962	11.92740	0.10	2.94
	6	0.03940	0.05920	11.82056	0.15	2.88
0	144	0.05137	0.06489	11.56448	0.14	3.09
	72	0.05272	0.06536	11.59660	0.09	3.04
	0*	0.05234	0.06507	11.55000	0.14	3.00

the F and A configuration is $\Delta E_{FA}=3$ mRy per unit cell. The orientation dependence of the total energy $E(\alpha)$ can be fit by a Fourier expansion

$$E(\alpha)=\sum_{m=0}^{\infty} J_m \cos^m \alpha. \tag{9}$$

The energy difference as a function of the angle between the layer magnetizations is given by

$$\Delta E(\alpha)=E(\alpha)-E(\pi)=J_1(1+\cos\alpha) \tag{10}$$

if we restrict our considerations to the first order term. J_1 describes the bilinear coupling and is equal to $0.5\,\Delta E_{FA}$ within this approximation. The function $\Delta E(\alpha)$ is also shown in Fig. 3. One can see that this simple model reproduces the angular dependence obtained by the *ab initio* calculation within a few percent of ΔE_{FA}. Most probably it means that the interlayer exchange coupling in Fe/Cr superlattices is dominated by bilinear coupling. Similar calculations have been performed by Freyss *et al.*[32] In difference to our results but in agreement with Slonczewski's proximity magnetism model[33] the authors obtain a parabolic dependence of the total energy with respect to the angles between the magnetization of successive Fe layers. This contradiction is related to the Cr spiral. In the calculations of Freyss *et al.*[32] the angle between the Fe and Cr interface moments is large whereas the angle between adjacent Cr moments is small. Consequently, the proximity magnetism model is applicable. In our calculations the angle between Cr moments is large since the Fe interface moments are included in the spiral. As a result the proximity magnetism model can not be applied and the total energy changes due to Eq. (10).

B. Transport properties

Concerning the conductivity components: The general trend is that the conductivities increase with increasing mag-

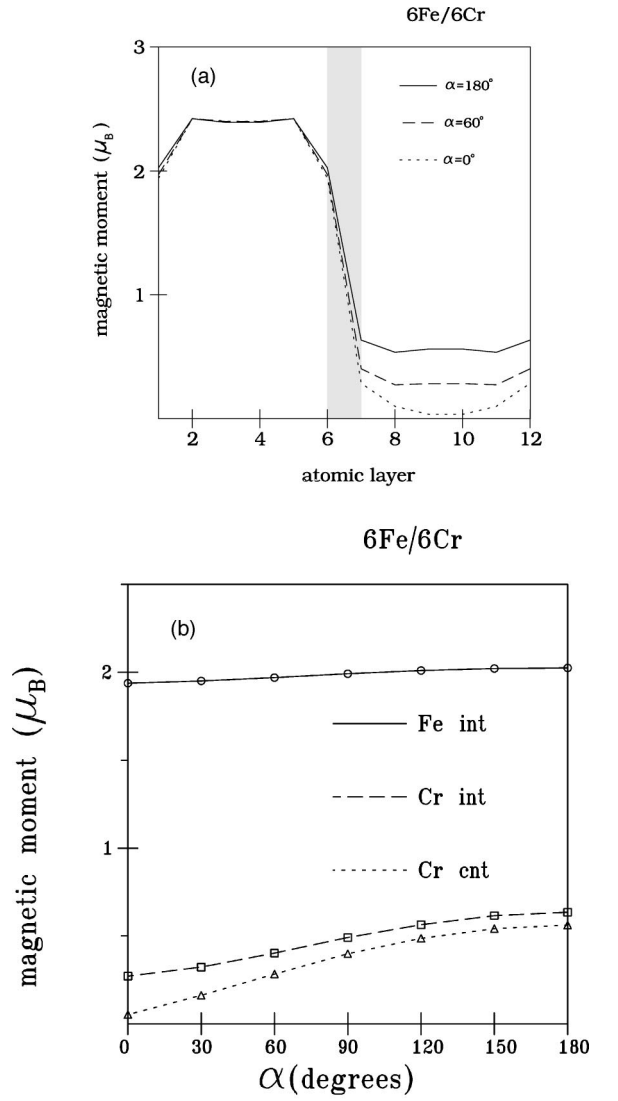

FIG. 2. Absolute values of the moments in 6Fe/6Cr superlattices: (a) Distribution of the moments in the unit cell for collinear, $\alpha=0$ and $\alpha=180°$, configurations, and for the noncollinear configuration with $\alpha=60°$. Atomic layers 1 to 6 correspond to Fe, atomic layers 7 to 12 correspond to Cr, the interface is indicated by a grey bar. (b) Variation of the moments with the angle of coupling between the Fe layers α for iron and chromium atomic layers at the interface, and for the atomic layer at the center of the Cr layer.

netic order between the Fe layers. This is found for CIP as well as for CPP conductivities. The CPP conductivities are in any case smaller than the CIP results but the relative change with the magnetic configuration is much stronger for CPP. Furthermore, if the conductivities are analyzed as a function of β, that is, the noncollinear order in the Cr layer we find the lowest conductivities always for nearly antiferromagnetic order which is the energetically favorable configuration. As can be seen from Table I and as was shown already before[11] the absolute values of the conductivities are not directly proportional to the density of states but rather reflect the influence of the anisotropic Fermi velocities in the layered system.

The calculated angular dependence of CIP- and CPP-GMR is shown in Fig. 4. If we would use the same expansion as for the energy difference for GMR

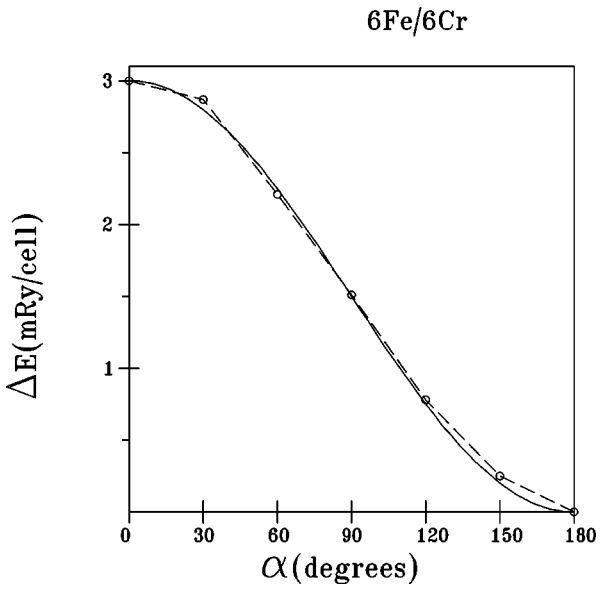

FIG. 3. Dependence of the total energy in 6Fe/6Cr superlattices on the angle of coupling between Fe layers. Circles show the calculated values, the broken line is a guide for the eyes. The solid line is the function $0.5\,\Delta E_{FA}(1+\cos\alpha)$ [see Eq. (10)].

$$\mathrm{GMR}(\alpha)=0.5\,\mathrm{GMR}_{FA}(1+\cos\alpha). \tag{11}$$

the result should be a straight line as a function of $\cos^2\alpha/2$. The deviations are a hint that higher order terms have to be included in the fit. At $\alpha=180°$ CIP-GMR is about 50%, which is in reasonable agreement with the experimental results obtained in Fe/Cr(001) superlattices with a chromium layer thickness of 9 Å.[2] The remarkable feature is that the maximum of the function occurs at $\alpha\neq180°$. The possibility of such a behavior was predicted in the model approach[13] under the condition that the spin asymmetry of the scattering

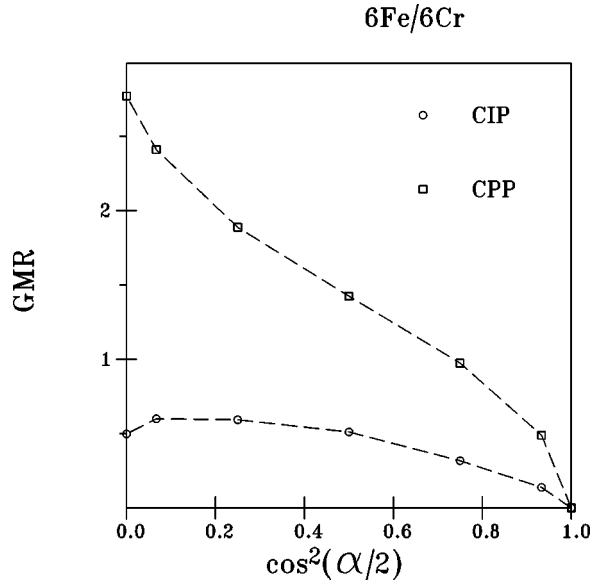

FIG. 4. Angular dependence of CIP- and CPP-GMR in a 6Fe/6Cr superlattice as a function of $\cos^2\alpha/2$. 0 corresponds to $\alpha=\pi$ and 1 to $\alpha=0$.

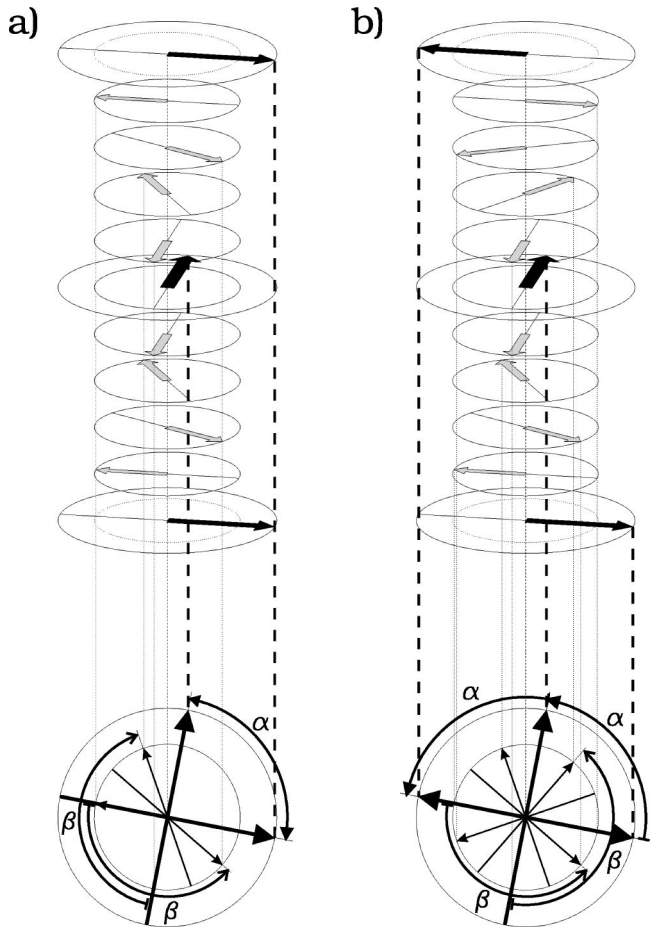

FIG. 5. Relative orientation of the magnetic moments in 2Fe/4Cr superlattices with (a) tilting and (b) spiral magnetic structure ($\alpha=90°, \beta=150°$).

potentials at the two successive interfaces differs significantly. It is interesting that the same result is obtained with constant relaxation times by taking into account the realistic potential landscape of the superlattices. For the CPP component the effect is much higher and at $\alpha=180°$ CPP-GMR is about 280%. A comparable difference between CIP and CPP was obtained experimentally by Gijs *et al.*[34] for Fe/Cr multilayers.

Finally we would like to discuss the question if the calculated spiral magnetic structures are applicable to describe the angular dependence of GMR. Indeed, the in-plane directed external magnetic field most likely leads to the appearance of a magnetic ordering referred to as ''tilting.'' Namely, in this configuration the angle of coupling between two neighboring iron layers is constant, while in every other Fe layer the directions of magnetization are again parallel. This fact leads to the doubling of the unit cell with respect to the nonmagnetic case. In order to verify this point we have carried out energy structure calculations for 2Fe/4Cr(001) superlattices with both spiral and tilting magnetic configurations. The differences between the tilting and the spiral structure at $\alpha=90°$, $\beta=150°$ are illustrated in Fig. 5. The angular dependence of CIP- and CPP-GMR is shown in Fig. 6. For the CIP component there is a fairly good agreement

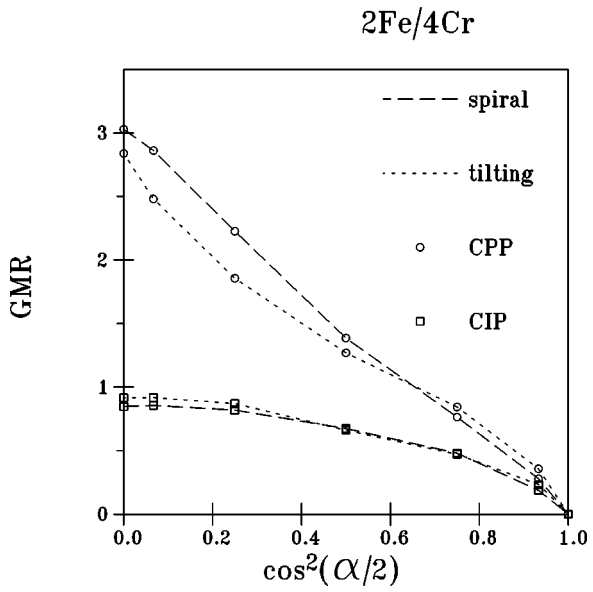

FIG. 6. Comparison of the angular dependence of CIP- and CPP-GMR in 2Fe/4Cr superlattices calculated for tilting and spiral magnetic structure.

within a few percent between the two configurations. For CPP-GMR at $\cos^2(\alpha/2)=0.25$ and 0.067 ($\alpha=120°$ and 150°, respectively) the difference is more pronounced (about 15%). Nevertheless, both curves behave in a very similar manner. That means, that the behavior of GMR is mainly determined by adjacent magnetic layers. Long-range magnetic order is less important. Consequently, the angular dependence of GMR computed on the basis of an electronic structure calculation with spiral magnetic order is fully valid and preferable. Because first of all, the doubling of the unit cell for the tilting configuration in comparison to the spiral leads to a considerable increase of the computational effort required to achieve self-consistency. Furthermore, the Fermi surface integration for the conductivity calculation requires a much denser **k** mesh to reach the same accuracy.

V. CONCLUSIONS

Self-consistent *ab initio* calculations of the electronic structure in 6Fe/6Cr superlattices with a spiral magnetic configuration have been performed for the first time. For the magnetic structure was assumed that Fe layers are intrinsically ferromagnetic and couple under an angle α to the adjacent Fe layer. The coupling at the Fe and Cr interface is fixed to be antiferromagnetic. The Cr moments form a spiral with constant angle. Comparing total energies, it was shown that at fixed angle of coupling between Fe layers, α, chromium moments tend to order antiferromagnetically. The calculated GMR is in reasonable agreement with experimental results. The remarkable feature of the calculated angular dependence is that we obtain differences in comparison to the assumed $\cos\alpha$ behavior both in CIP and CPP configuration which seems to be specific in Fe/Cr since it was not so pronounced in Co/Cu.[14] Finally we have shown that an assumed spiral structure leads to the same results for the orientation dependence of GMR as the more realistic tilting mode.

*Permanent address: Institute for Metal Physics, Kiev, Ukraine.
[1] P. Grünberg, R. Schreiber, Y. Pang, M.B. Brodsky, and H. Sowers, Phys. Rev. Lett. **57**, 2442 (1986).
[2] M.N. Baibich, J.M. Broto, A. Fert, F. Nguyen Van Dau, F. Petroff, P. Etienne, G. Creuzet, A. Friederich, and J. Chazelas, Phys. Rev. Lett. **61**, 2472 (1988).
[3] G. Binash, P. Grünberg, F. Saurenbach, and W. Zinn, Phys. Rev. B **39**, 4828 (1989).
[4] P.M. Levy, S. Zhang, and A. Fert, Phys. Rev. Lett. **65**, 1643 (1990); S. Zhang, P.M. Levy, and A. Fert, Phys. Rev. B **45**, 8689 (1992).
[5] R.Q. Hood and L.M. Falicov, Phys. Rev. B **46**, 8287 (1992).
[6] T. Valet and A. Fert, Phys. Rev. B **48**, 7099 (1993).
[7] B. Dieny, V.S. Speriosu, S.S.P. Parkin, B.A. Gurney, D.R. Wilhoit, and D. Mauri, Phys. Rev. B **43**, 1297 (1991).
[8] B.H. Miller, B.P. Stojkovic, and E.D. Dahlberg, Phys. Lett. A **256**, 294 (1999).
[9] T. Oguchi, J. Magn. Magn. Mater. **126**, 519 (1993).
[10] K.M. Schep, P.J. Kelly, and G.E.W. Bauer, Phys. Rev. Lett. **74**, 586 (1995).
[11] P. Zahn, I. Mertig, M. Richter, and H. Eschrig, Phys. Rev. Lett. **75**, 2996 (1995).
[12] S. Zhang, P.M. Levy, and A. Fert, Phys. Rev. B **45**, 8689 (1992).
[13] J. Barnas, O. Baksalary, and A. Fert, Phys. Rev. B **56**, 6079 (1997).
[14] C. Blaas, P. Weinberger, L. Szunyogh, J. Kudrnovský, V. Drchal, P.M. Levy, and C. Sommers, Eur. Phys. J. B **9**, 245 (1999).
[15] L.B. Steren, A. Barthelemy, J.L. Duvail, A. Fert, R. Morel, F. Petroff, P. Holody, R. Loloee, and P.A. Schroeder, Phys. Rev. B **51**, 292 (1995).
[16] P. Dauguet, P. Gandit, J. Chaussy, S.F. Lee, A. Fert, and P. Holody, Phys. Rev. B **54**, 1083 (1996).
[17] B. Dieny, C. Cowache, A. Nossov, P. Dauguet, J. Chaussy, and P. Gandit, J. Appl. Phys. **79**, 6370 (1996).
[18] A. Schreyer, C.F. Majkrzak, Th. Zeidler, T. Schmitte, P. Bödeker, K. Theis-Bröhl, A. Abromeit, J. Dura, and T. Watanabe, Phys. Rev. Lett. **79**, 4914 (1997).
[19] R.S. Fishman, Phys. Rev. Lett. **81**, 4979 (1998).
[20] D.T. Pierce, J. Unguris, R.J. Celotta, and M.D. Stiles, J. Magn. Magn. Mater. **200**, 290 (1999).
[21] H. Zabel, J. Phys.: Condens. Matter **11**, 9303 (1999).
[22] L.M. Sandratskii, Phys. Status Solidi B **135**, 167 (1986).
[23] Kübler, K.-H. Hock, J. Sticht, and A.R. Williams, J. Appl. Phys. **63**, 3482 (1988).
[24] L.M. Sandratskii, Adv. Phys. **47**, 91 (1998).
[25] S.V. Halilov, H. Eschrig, A.Y. Perlov, and P.M. Oppeneer, Phys. Rev. B **58**, 293 (1998).
[26] C. Herring, *Magnetism*, edited by G. Rado and H. Suhl (Academic Press, New York, 1966), Vol. IV, p. 407.
[27] L.M. Sandratskii, J. Phys.: Condens. Matter **3**, 8565 (1991).
[28] O.K. Andersen, Phys. Rev. B **12**, 3060 (1975).
[29] J. Binder, P. Zahn, and I. Mertig, J. Appl. Phys. **87**, 5182 (2000).
[30] S.S.P. Parkin, N. More, and K.P. Roche, Phys. Rev. Lett. **64**, 2304 (1990).
[31] P.E. Blöchl, O. Jepsen, and O.K. Andersen, Phys. Rev. B **49**, 16 223 (1994).
[32] M. Freyss, D. Stoeffler, and H. Dreyssé, Phys. Rev. B **54**, 12 677 (1996).
[33] J.C. Slonczewski, J. Magn. Magn. Mater. **150**, 13 (1995).
[34] M.A.M. Gijs, S.K.J. Lenczowski, and J.B. Giesbers, Phys. Rev. Lett. **70**, 3343 (1993); M.A.M. Gijs, S.K.J. Lenczowski, J.B. Giesbers, R.J.M. van de Veerdonk, M.T. Johnson, R.M. Jungblut, A. Reinders, and R.M.J. van Gansewinkel, J. Magn. Magn. Mater. **151**, 333 (1995).